Interatomic potentials of van der Waals dimers Hg_2 and Cd_2: Probing discrepancies between theory and experiment

T Urbańczyk[1], M Krośnicki[2], M Strojecki[3], A Pashov[4], A Kędziorski[5], P Żuchowski[5] and J Koperski[1]

[1] Smoluchowski Institute of Physics, Jagiellonian University, prof. S. Łojasiewicza 11, 30-348 Kraków, Poland
[2] Institute of Theoretical Physics and Astrophysics, University of Gdansk, Wita Stwosza 57, 80-952 Gdańsk, Poland
[3] Jerzy Haber Institute of Catalysis and Surface Chemistry, Polish Academy of Sciences, Niezapominajek 8, 30-239 Kraków, Poland
[4] Department of Physics, Sofia University, 5 James Bourchier Boulevard, 1164 Sofia, Bulgaria
[5] Institute of Physics, Nicolaus Copernicus University, Grudziądzka 5/7, 87-100 Toruń, Poland

E-mail: ufkopers@cyf-kr.edu.pl

Abstract. Results of new all-electron *ab initio* calculations and revisit of experimental studies of the interatomic potentials of lower-lying *ungerade* excited and ground electronic energy states of the Hg_2 and Cd_2 van der Waals complexes are used as probes of discrepancies between theory and experiment. From simulations of the previously and presently measured LIF excitation and dispersed emission spectra new analytical representations of the excited- and the ground-state interatomic potentials are proposed. An inverted perturbation approach was also used to improve the studied interatomic potentials. The comparison of the new *ab-initio* calculated potentials with the results of the analyses illustrates an improve theory-to-experiment agreement for such a demanding system like Hg_2 or Cd_2.

1. The objective of the study

The main objective of the study presented here was calculation of new all-electron *ab initio* interatomic potentials for the Hg_2 and Cd_2 lower-lying *ungerade* excited and the ground states, and their subsequent assessment against the potentials that are the result of analyses of newly recorded and re-analyses of previously recorded experimental spectra using pulsed and continuous supersonic beams [1–9]. Some of the previous analyses were performed using limited resources (*e.g.*, simulation procedures only for low v' and v'', and with only a Morse representation of interatomic potentials in their bound region), and without systematic consideration of the isotopic composition and rotational energy structures that otherwise can completely change results of the simulation (*e.g.*, intensities of the vibrational bands and their shapes). Consequently, in order to achieve the objective, the following agenda was realized:

- New all-electron *ab initio* calculations of the interatomic potentials for the lowest *ungerade* and the ground states of Hg_2 and Cd_2. These was executed to improve the theory-to-experiment agreement;
- Analysis of the newly recorded and revisit of the previously measured experimental spectra in

order to perform simulations of the LIF excitation and LIF dispersed emission spectra using programs and procedures that were originally omitted due to their unavailability *i.e.*, LeRoy's LEVEL [10] and BCONT [11] as well as Western's PGOPHER [12];

- Implementation of analytical representations for the Hg_2 and Cd_2 lowest *ungerade*- and ground-state potentials as well as point-wise representations, obtained using the IPA method [13] for which an analytical representation was found to be impossible;
- Comparison of new *ab-initio* calculated potentials with results of new measurements and new analyses as well as with other *ab initio* calculations and experimental results.

2. Computational results: *ab initio* calculations of Hg_2 and Cd_2 interatomic potentials

The all-electron *ab initio* calculations were performed using the MOLCAS 8.0 package [14]. Details of the calculations for Hg_2 are given in [15].

For Cd_2 Atomic Natural Orbitals (ANO-RCC) basis set was used as designed by Roos *et al.* [16]. The basis set was formed from 21*s*19*p*13*d*6*f*4*g*2*h* Gaussians contracted as 10*s*8*p*8*d*6*f*4*g*2*h* and it allowed for correlation of semi core electrons.

The Hamiltonian used in electron correlation calculations was spin-free second-order Douglas-Kroll-Hess (D-K-H) Hamiltonian [17,18] which accounted for scalar relativistic effects. In order to account for static correlations, complete-active-space self-consistent-field (CASSCF) [19-21] calculations were performed. In the CASSCF calculations molecular orbitals and configuration interaction coefficients of the wave functions were simultaneously optimized. The active space was formed by distributing four active electrons on molecular counterparts of atomic orbitals Cd-5*s*, Cd-5*p* and Cd-6*s*. All closed orbitals were optimized. As starting orbitals, canonical Hartree-Fock orbitals were used. The starting dimension of the small configuration interaction (CI) matrix in the Davidson procedure for the $X^1\Sigma_g^+$ and $(1)^1\Sigma_u^+$ states was set to two; and for the $(1)^3\Sigma_u^+$ state it was set to three [(1) denotes first on the energy scale of the electronic energy state with the given symmetry]. This avoided convergence problems for short interatomic distances. The molecular orbitals and wave functions were optimized in CASSCF calculations separately for each molecular excited electronic state of *ungerade* symmetry that originated from the 5*s*6*p* atomic configuration, with only one exception in case of $(1)\Pi_u$ state which was optimized simultaneously with second state of this symmetry (having ionic character) due to strong configuration interaction.

In the second step, dynamic electron correlations using restricted active space multi-state second-order perturbation theory calculations (MS-CASPT2) [22-25] were included. In CASPT2 calculations, 24 electrons (4 active and 20 closed-shell) were fully correlated. The active space was the same as on the level of CASSCF theory. The 10 molecular counterparts of atomic 5*d* orbitals were correlated through single and double excitations. The rest of core orbitals were not optimized and kept frozen.

In the last step, spin-orbit (S-O) coupling effects were included by means of restricted-active space state-interaction spin-orbit (RASSI-SO) calculations [26]. In this step, many-electron Hamiltonian with the s-o coupling terms of the second-order D-K-H Hamiltonian [17,18] were supplemented and the atomic mean-field approximation (AMFI) for their integrals [27] was adopted. In the RASSI code S-O matrix element were calculated in a wave function basis which is formed from individually optimized CI expansions in the previous CASSCF/CASPT2 calculations. All *ungerade* triplet and singlet states originating from $(5s5p)^3$P Cd and $(5s5p)^1$P Cd configuration, as well as the ground state were included in this step. The transition dipole moments (TDM) were determined within RASSI by calculation the interaction matrix elements between the ground and the excited states.

3. Experimental results: spectroscopy of Hg_2 and Cd_2 in supersonic beams

Laser spectroscopy of 12-group vdW complexes produced and ro-vibrationally cooled in a free-jet expansion beams is one of methods for investigation of molecular energy structure [1]. It has been applied, among others, in experimental studies of the lower-lying $E^3 1_u(6^3P_2)$-, $F^3 0_u^+(6^3P_1)$-, $D^3 1_u(6^3P_1)$- and $G^1 0_u^+(6^1P_1)$-state interatomic potentials of Hg_2, and $A^1 0_u^+(5^1P_1)$-, $B^1 1_u(5^1P_1)$-, $a^3 1_u(5^3P_1)$-, $b^3 0_u^+(5^3P_1)$- and $c^3 1_u(5^3P_2)$-state interatomic potentials of Cd_2 excited, and the $X^1 0_g^+$ ground electronic-energy states

of Hg_2 and Cd_2. Details of the experiments for Hg_2 are given in [15] while for the Cd_2 are reported in [2-9].

4. Results and discussion

As an example of results, analysis of the LIF excitation spectrum recorded using the $A^1 0_u^+ \leftarrow X^1 0_g^+$ transition in Cd_2 is presented. The excitation spectrum consists of the $v' \leftarrow v''=0$ progression with v' spanning the range from $v'=18$ to 53. As can be seen in Fig. 1a, the approximate locations of the excited v' are in the lower half of the $A^1 0_u^+$ -state potential well *i.e.*, closer to the bottom of the well than to the dissociation limit.

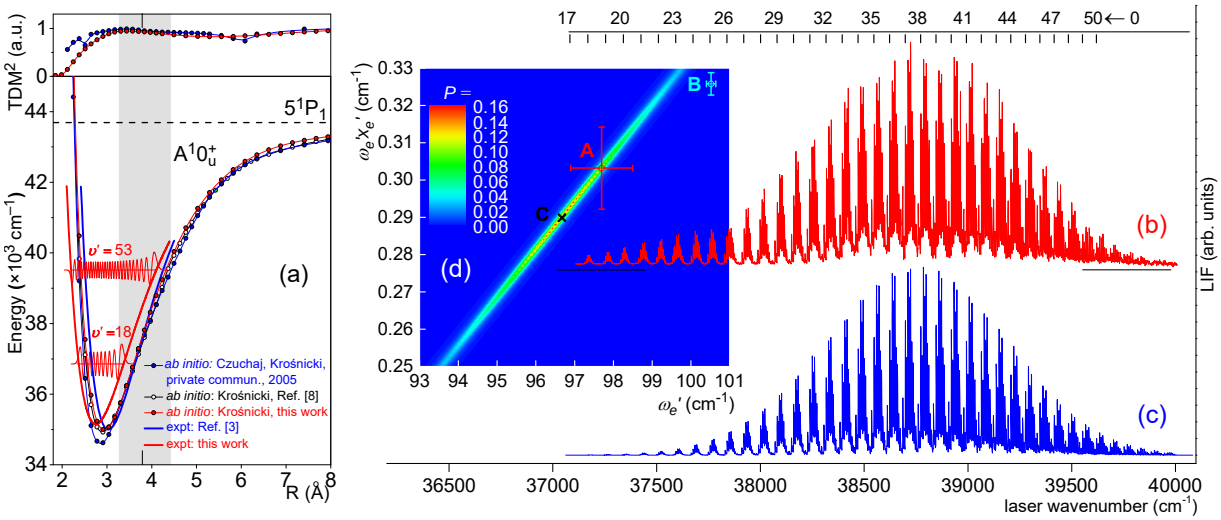

Figure 1. (a) Interatomic potential of the $A^1 0_u^+$ state of Cd_2. The determined TDM^2 (normalized) of Czuchaj and Krośnicki and of this study are shown in the upper. Grey area: Franck-Condon window for excitation from $v''=0$. Vertical lines: position of the R_e'' =3.76 Å. (b) LIF excitation spectrum recorded previously [3] using the $A^1 0_u^+ \leftarrow X^1 0_g^+$ transition. (c) Simulation [10,12] performed assuming shifted (−656.9 cm^{-1}) Morse representation of the $A^1 0_u^+$ -state potential (D_e'=7882.5 cm^{-1}, β' = 1.0072 $Å^{-1}$, R_e' = 2.75 Å, see part 1a). For the $X^1 0_g^+$-state potential, a L-J(n−6)-Morse representation (D_e'' = 328 cm^{-1}, R_e'' = 3.76 Å, n = 3.86) was used; the TDM^2 of this study was included. (d) The ω_e'-$\omega_e'x_e'$ *agreement plot* drawn using vibrational transition energies $E_{v'}$ of the most abundant $^{114}Cd^{112}Cd$ isotopologue recorded in the spectrum. The simulation-to-experiment agreement [parameter P, see text] in function of the ω_e' and $\omega_e'x_e'$ is presented using a colour scale. Point A corresponds to the ω_e' and $\omega_e'x_e'$ and their uncertainties obtained as a result of this work (ω_e' = 97.74 cm^{-1} and $\omega_e'x_e'$ = 0.303 cm^{-1}). Point B shows the ω_e' and $\omega_e'x_e'$ and their uncertainties reported in [3]. Center of the plot (point C) is the ω_e' and $\omega_e'x_e'$ for which one obtains the best simulation-to-experiment agreement in the analysis of the excitation spectrum.

4.1. The agreement plot

Re-analysis of LIF excitation spectrum recorded using the $A^1 0_u^+ \leftarrow X^1 0_g^+$ transition [3] shown in Fig. 1b began with employing of so-called *agreement plot* method *via* examination of the $E_{v'}^{\ expt}$ energies of vibrational transition recorded in the spectrum for the most abundant $^{114}Cd^{112}Cd$ isotopologue. The *agreement plot* illustrates a new method of determination of pairs of the ω_e' and $\omega_e'x_e'$ vibrational constants. The method is used under an assumption that in the region of the recorded $E_{v'}^{\ expt}$, the $A^1 0_u^+$ -state potential is represented by a Morse function. The main advantage of the method [in comparison to well-known Birge–Sponer (B–S) plot] is acknowledging the fact that vibrational constants ω_e' and $\omega_e'x_e'$ are highly correlated. In other words, it can be shown that there are exist many of the (ω_e' , $\omega_e'x_e'$) pairs which can be used to perform simulations that are in satisfactory agreement with the experimental spectrum, especially when the rotational structure of the spectrum is not resolved.

For each combination of the ω_e' and $\omega_e'x_e'$ in the specified ranges of their values (*e.g.*, around their expected values obtained using the B–S plot), the corresponding $A^1 0_u^+$ -state Morse representation was determined. Next, for each Morse representation using the LEVEL, $E_{v'}^{sim}$ energies of the vibrational transitions corresponding to the transitions observed in the experimental spectrum were calculated. Then, the $E_{v'}^{sim}$ were compared with the recorded $E_{v'}^{expt}$. Finally, for each Morse representation, the so-called *agreement coefficient* $P = 1/(0.01+\chi^2)$ was calculated, where $\chi^2 = \Sigma_{v'}(\Delta E_{v'}^{exp} - \Delta E_{v'}^{sim})^2$ is a sum of squares of the differences between $\Delta E_{v'}^{expt}$ experimental and $\Delta E_{v'}^{sim}$ simulated energy separations, and $\Delta E_{v'}^{sim} = E_{v'}^{sim} - E_{int\,v'}^{sim}$, where $E_{int\,v'}^{sim}$ is an energy of the selected *e.g.*, more intense, $v' \leftarrow v''=0$ transition in the experimental spectrum; the $\Delta E_{v'}^{expt}$ were calculated similarly to the $\Delta E_{v'}^{sim}$. The coefficient P describes the agreement between the simulation and experimental results in a quantitative way.

4.2. The spectrum

The *agreement plot i.e.*, a contour plot of the agreement coefficient P in function of the ω_e' and $\omega_e'x_e'$ is shown in Fig. 1d. As one can see, the (ω_e', $\omega_e'x_e'$) pair obtained in [3] depicted with cross B (also representing error bars) is located out of the area where the P gains high values. In the *plot*, the result of this study (ω_e' =97.74 cm^{-1}, $\omega_e'x_e'$ =0.303 cm^{-1}) is depicted with cross A. Centre of the *plot* (see cross C) that gives the best simulation-to-experiment agreement (ω_e' =96.65 cm^{-1}, $\omega_e'x_e'$ =0.29 cm^{-1}) does not match the values accepted in this study. This is caused by the result of simulation of LIF dispersed emission spectrum [3].

We focused our attention at simulation of the LIF excitation spectrum previously recorded using the $A^1 0_u^+ \leftarrow X^1 0_g^+$ transition (Fig. 1b). Due to the high values of v', the isotopic structure in each of the vibrational components was easily resolved. In previous simulation of the excitation spectrum [3] neither an influence of TDM nor rotational structure of the $v' \leftarrow v''=0$ components has been taken into account.

Simulation of the excitation spectrum began with an assumption of a Morse representation for the $A^1 0_u^+$ state and with the (ω_e', $\omega_e'x_e'$) pair as concluded from the *agreement plot* (cross C). However, parallelly performed simulation of LIF dispersed emission spectrum from [3] indicated that, despite the simulation-to-experiment agreement was high, the (ω_e', $\omega_e'x_e'$) pair chosen from the centre of the *agreement plot* is not the best choice as far as both simulations are concerned. Consequently, other (ω_e', $\omega_e'x_e'$) pair was selected (cross A). It is necessary to emphasize that in the (ω_e', $\omega_e'x_e'$) selection process, a trend towards the result of [3] together with high values of P was preferred. In the simulation procedure described in details elsewhere [9], LEVEL 8.0 and PGOPHER 8.0 were employed, taking into account the *full* isotopic composition of Cd_2 as well as rotational energy structure of the $^1\Sigma_u^+ \leftarrow {}^1\Sigma_g^+$, $\Omega'=0 \leftarrow \Omega''=0$ transition. An influence of TDM squared calculated in this work (see upper part in Fig. 1a) was also included in the simulation. Result is shown in Fig. 1c. It can be verified that a correct distribution of intensities of Cd_2 isotopologues has been reconstructed what was not achieved in previous study [3]. Another conclusion that came from the simulation was a lack of strong influence of TDM squared as the TDM has almost constant values for R for which the transition takes place (see Franck-Condon window for excitation in Fig. 1a, grey area).

5. Summary

The objective formulated in Sec. 1 was realized. Specific points are the following.

- New all-electron *ab initio* calculations of the $E^3 1_u$, $F^3 0_u^+$, $D^3 1_u$ and $G^1 0_u^+$-state interatomic potentials of Hg_2, and $A^1 0_u^+$, $B^1 1_u$, $a^3 1_u$, $b^3 0_u^+$ and $c^3 1_u$-state interatomic potentials of Cd_2 were performed in order to improve the theory-to-experiment agreement. Indeed, a significant improvement and increased agreement with the experimental interatomic potentials were achieved as compared to the earlier calculations.
- Presently and previously recorded LIF excitation and LIF dispersed emission spectra were analyzed or revisited, and their simulations were performed employing the LEVEL 8.0, BCONT 2.2 and PGOPHER 8.0 programs. The full isotopic composition of Hg_2 and Cd_2, as well as the rotational energy structure of their transitions were taken into account.

● New analytical representations of the Hg_2 and Cd_2 lowest excited *ungerade*-state potentials, *i.e*. Morse, Morse-vdW or ground-state potentials, *i.e*. Morse-L–J(n–6) or Morse-L–J(n–m) were obtained. For the $D^3\Pi_u$ and $G^1\Pi_g$ electronic states of Hg_2 the new representations were obtained using an inverted perturbation approach (IPA).

● A comparison of the new *ab initio* calculated potentials with results of new analyses as well as other *ab initio* calculations was performed. These comparisons illustrate an improved theoretical and experimental characterization of the lowest excited *ungerade*- and ground-state potentials of Hg_2 and Cd_2.

Acknowledgements
This work was supported by the National Science Centre Poland under grant number UMO-2015/17/B/ST4/04016.

References

[1] Koperski J 2002 *Phys Rep.* **369** 177
[2] KoperskiJ, Łukomski M and Czajkowski M 2002 *Spectrochim. Acta A* **58** 927
[3] Łukomski M, Koperski J, Czuchaj E and Czajkowski M 2003 *Phys. Rev. A* **68** 042508
[4] Łukomski M, Ruszczak M, Czuchaj E and Koperski J 2005 *Spectrochim. Acta A* **61** 1835
[5] Strojecki M, Ruszczak M, Łukomski M and Koperski J 2007 *Chem. Phys.* **340** 171
[6] Ruszczak M, Strojecki M, Łukomski M and Koperski J 2008 *J. Phys. B: At. Mol. Opt. Phys.* **41** 245101
[7] Strojecki M, Krośnicki M, Zgoda P and Koperski J 2010 *Chem. Phys. Lett.* **489** 20
[8] Koperski J, Strojecki M, Krośnicki M and Urbańczyk T 2011 *J. Phys. Chem. A* **115** 6851
[9] Urbańczyk T and Koperski J 2014 *Mol. Phys.* **114** 2486
[10] LeRoy R J 2002 *LEVEL 8.0 A Computer Program for Solving the Radial Schrödinger Equation for Bound and Quasibound Levels* (University of Waterloo Chemical Physics Research Report) CP-655R
[11] LeRoy R J, Kraemer G T 2004 *BCONT 2.2 A Computer Program for calculating Bound→ Continuum Transition Intensities for Diatomic Molecules* (University of Waterloo Chemical Physics Research Report) CP-650R2
[12] Western C M 2013 *PGOPHER 8.0, a Program for Simulating Rotational Structure* (University of Bristol)
[13] Pashov A, Jastrzębski W and Kowalczyk P 2000 *Comput. Phys. Commun.* **128** 622
[14] Karlström G, Lindh R, Malmqvist P-Å, Roos B O, Ryde U, Veryazov V, Widmark P O, Cossi M, Schimmelpfennig B, Neogrady P and Seijo L 2003 *Comput. Mater. Sci.* **28** 222
[15] Krośnicki M, Strojecki M, Urbańczyk T, Pashov A and Koperski J 2015 *Phys. Rep.* **591** 1
[16] Roos B O, Lindh R, Malmqvist P-Å, Veryazov V and Widmark P-O 2005 *J. Phys. Chem. A* **109** 6575
[17] Douglas M and Kroll N M 1974 *Ann. Phys. (N.Y.)* **82** 89
[18] Hess B A 1986 *Phys. Rev. A* **33** 3742
[19] Roos B O, Taylor P R and Siegbahn P E M 1980 *Chem. Phys.* **48** 157
[20] Siegbahn P E M, Heiberg A, Roos B O and Levy B 1980 *Phys. Scr.* **21** 323
[21] Siegbahn P E M, Heiberg A, Almlöf J and Roos B O 1981 *J. Chem. Phys.* **74** 2384
[22] Andersson K, Malmqvist P-Å, Roos B O, Sadlej A J and Wolinski K1990 *J. Phys. Chem.* **94** 5483
[23] Andersson K, Malmqvist P-Å and Roos B O 1992 *J. Chem. Phys.* **96** 1218
[24] Zaitsevskii A and Malrieu J P 1995 *Chem. Phys. Lett.* **233** 597
[25] Finley J, Malmqvist P-Å, Roos B O and Serrano-Andrés L 1998 *Chem. Phys. Lett.* **288** 299
[26] Malmqvist P-Å, Roos B O and Schimmelpfennig B 2002 *Chem. Phys. Lett.* **357** 230
[27] Hess B A, Marian C M, Wahlgren U and Gropen O 1996 *Chem. Phys. Lett.* **251** 365